theoretical rate constants for the polarization and locked-dipole limits. Recent work[17] has shown that this phenomenon is often observed for ion–molecule reactions, involving polar neutrals, and that the observed rate constant is generally closer to the polarization limit, indicating that the effect of the dipole moment is to a large extent averaged out by molecular rotation of the neutral molecule.

In contrast to the general observation, the reactions of the CH_3^+ and CH_2^+ ions, which proceed mainly by condensation, exhibit rates even less than the polarization limit. An apparent exception is the CH_2^+–NH_3 reaction. This observation tends to support the idea[10] that significant barriers to some dissociation channels of intermediate complexes in ion–molecule reactions may exist as a result of the large amount of molecular rearrangement required to form condensation products. The result is simply back reaction where no other exothermic reaction channels are available. Also, comparison of the observed reactions in CH_4–H_2S *vs.* CH_4–H_2O mixtures, and in CH_4–NH_3 *vs.* CH_4–PH_3[18] mixtures, shows that a larger number of condensation reactions are observed in mixtures with second-row hydrides compared with hydrides of the first-row elements. Rearrangement apparently occurs more readily in reactions involving ions and neutrals of the larger second-row hydrides.

The most surprising observation to be made from Table XI is that the reactions of the hydride ions with methane are so slow, the apparent exception in this case being the H_2O^+–CD_4 reaction. A possible explanation is that there are no exothermic proton-transfer or charge-transfer reaction channels available in these reactions (the OH^+ ion being the exception in this instance). The exothermic reaction channels for these reactions consist of abstraction reactions (of H_2, H, or H^- from the neutral) and condensation reactions. Abstraction reactions all seem to exhibit slow rates when observed at all (again the H_2O^+–CD_4 reaction excepted), and evidence has already been presented for the existence of barriers to condensation reactions.

Acknowledgment. The authors wish to acknowledge the work of M. Mosesman who provided the initial impetus in the initial stages of these studies.

(17) T. Su and M. T. Bowers, *J. Chem. Phys.*, in press.
(18) D. Holtz, J. L. Beauchamp, and J. R. Eyler, *J. Amer. Chem. Soc.*, **92**, 7045 (1970).

Mechanism for Scrambling and Dissociation of Short-Lived Intermediate in a Crossed-Beam Reaction of Methyl Cation and Methane

John Weiner,* G. P. K. Smith, Martin Saunders, and R. J. Cross, Jr.

Contribution from the Department of Chemistry, Yale University, New Haven, Connecticut 06520. *Received June 12, 1972*

Abstract: Crossed-beam studies of the ion–molecule reaction $CD_3^+ + CH_4 \rightarrow C_2X_5^+ + X_2$ (X = H, D) and its isotopic complement $CH_3^+ + CD_4 \rightarrow C_2X_5^+ + X_2$ (X = H, D) yield the following results. (a) All $C_2X_5^+$ products arise from a direct reaction mechanism with no evidence of long-lived intermediate formation. (2) Total reaction cross sections calculated from probability contour plots show a marked trend toward nonrandom H, D scrambling with increasing collision energy. A kinetic model of scrambling and dissociation in the short-lived intermediate is proposed to account for the results.

Although Herman, *et al.*,[1] have convincingly demonstrated that the reaction of methyl cation with methane does not proceed through a long-lived intermediate, the mechanism is still far from clear since tandem mass spectrometer (TMS)[2] and ion cyclotron resonance (icr)[3] studies both show extensive H–D scrambling in isotopically labeled products. A possible inference is that the $C_2H_ND_{7-N}^+$ intermediate exists as a structural entity long enough for exchange to take place (a few vibrational periods) but not long enough to exist as a persistent collision complex[4] (a few rotational periods).

Here we report studies of two isotopic systems

$$CD_3^+ + CH_4 \longrightarrow C_2H_ND_{5-N}^+ + H_{4-N}D_{N-2} \quad (N = 2, 3, 4) \quad (1a)$$

$$CH_3^+ + CD_4 \longrightarrow C_2H_{5-N}D_N + H_{N-2}D_{4-N} \quad (N = 2, 3, 4) \quad (1b)$$

using the crossed-beam electron volt accelerator (EVA).[5] Our purpose in studying this system is twofold: first, to determine if reactions 1a and 1b proceed *via* a direct mechanism for all isotopic products or whether some products are formed in, say, a "stripping" mechanism[5] while others are formed through a long-lived interme-

(1) Z. Herman, P. Hierl, A. Lee, and R. Wolfgang, *J. Chem. Phys.*, **51**, 454 (1969).
(2) F. P. Abramson and J. H. Futrell, *J. Chem. Phys.*, **45**, 1925 (1966).
(3) W. T. Huntress, Jr., *J. Chem. Phys.*, **56**, 5111 (1972).
(4) A persistent collision complex is defined as an intermediate which lives long enough to scramble completely the *momenta* of the reactant species so that memory of the initial orientation of the momenta is completely lost to the products. Total linear momentum, of course, is conserved. Note the distinction between momentum scrambling and chemical (hydrogen–deuterium) scrambling. For an example of a persistent complex in ion–molecule reactions, see Z. Herman, A. Lee, and R. Wolfgang, *J. Chem. Phys.*, **51**, 452 (1969). See also W. B. Miller, S. A. Safron, and D. R. Herschbach, *Discuss. Faraday Soc.*, **No. 44**, 108 (1967), for a discussion of persistent collision complexes in thermal neutral–neutral reactions.
(5) Z. Herman, J. D. Kerstetter, T. L. Rose, and R. Wolfgang, *Discuss. Faraday Soc.*, **No. 44**, 123 (1967).

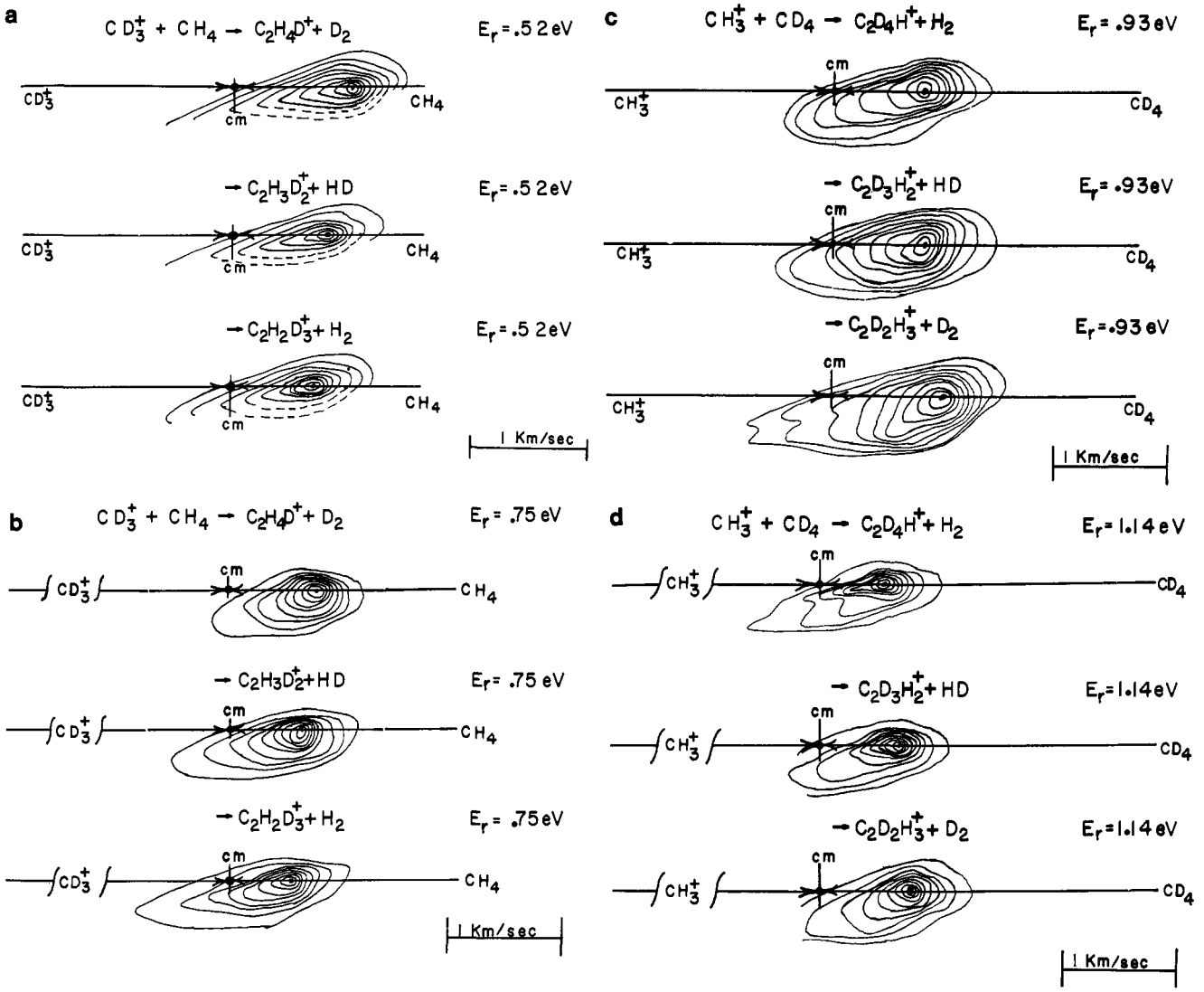

Figure 1. Probability contour plots for $C_2H_ND_{5-N}^+$ ($N = 1, 2, 3, 4$) in a Cartesian velocity space. Each plot is separately normalized to its peak value. Note that product translational energy in CM coordinates decreases with increasing collision energy (an indication of greater internal excitation). In a and b note that product distributions are progressively peaked further backward from $C_2H_4D^+$ to $C_2H_2D_3^+$, consistent with linear momentum conservation and the assumption of similar energy partitioning in all three isotopic products. Products $C_2HD_4^+$ to $C_2H_3D_2^+$ in c and d also show the expected trends.

diate. Previous crossed-beam work[1] with unlabeled product ions leaves open the possibility that the observed intensity contours are really the superposed results of two or more reaction mechanisms with a direct process predominating.

Our second objective is to study the relative distributions of isotopically labeled product ions as a function of collision energy. At near-thermal collision energies one might expect the rate of hydrogen–deuterium scrambling in the $C_2H_ND_{7-N}^+$ intermediate to be fast relative to the rate of decomposition. Consequently, a random distribution of isotopically labeled ion products would result. As the relative velocity of the incoming particles is increased, however, hydrogen–deuterium scrambling will have less time to "equilibrate" and nonrandom distributions in the products may be expected. The *specific* nonrandom behavior supplies important clues to the detailed nature of the reaction mechanism. One may propose kinetic models of the scrambling–dissociation process which, in turn, may provide evidence in support of structural models for hypercoordinated carbonium ion intermediates in chemical reactions.

Experimental Section

A detailed description of the EVA apparatus can be found elsewhere.[6] For the sake of clarity, however, a brief description follows. Methyl cations are produced in a conventional electron bombardment source. The ions emerge from the source and enter a 180° magnetic mass selector. Only ions with the proper mass-to-charge ratio are permitted to continue through the mass selector and into an electrostatic lens system which focuses and decelerates the beam to the desired laboratory energy. Immediately after leaving the lens system the ion beam enters a field-free interaction region where it intersects the collimated neutral beam at a 90° angle. The mass, angular, and translational energy distribution of the ion products is subsequently measured, and the data are presented in the form of probability contours in a Cartesian velocity space.[7]

In the case of reaction 1a, a possible ambiguity in the identification of the product $C_2H_4D^+$ arises since the secondary decomposition product $C_2D_3^+$ has the same mass-to-charge ratio. The reaction

$$CD_3^+ + CH_4 \longrightarrow C_2X_3^+ + X_2 + X_2 \qquad X = H, D$$

is endothermic by about 1.2 eV, and the highest collision energy we

(6) Z. Herman, J. D. Kerstetter, T. L. Rose, and R. Wolfgang, *Rev. Sci. Instrum.*, 40, 538 (1969).
(7) R. Wolfgang and R. J. Cross, Jr., *J. Phys. Chem.*, 73, 743 (1969).

have studied lies about 0.5 eV above this threshold for $C_2D_3^+$ formation (see Figure 2a). We may estimate the importance of $C_2D_3^+$ contamination in reaction 1a, however, by examining the intensity of $C_2H_3^+$ ions produced in reaction 1b. In the latter case no ambiguity between $C_2X_5^+$ and $C_2X_3^+$ (X = H, D) products arises since a unique mass-to-charge ratio exists for every isotopic species. The two reactant systems, 1a and 1b, are complementary so that it is reasonable to assume that the fractional cross section, $C_2D_3^+/(C_2H_4D^+ + \Sigma C_2X_3^+)$, in system 1a will be equal to the fractional cross section, $C_2H_3^+/(C_2HD_4^+ + \Sigma C_2X_3^+)$, in system 1b at the same relative collision energy. Here $\Sigma C_2X_3^+$ denotes a sum over all $C_2X_3^+$ (X = H, D) isotopic products. We have verified this assumption directly by calculating the $C_2X_3^+$ fractional cross sections for those isotopic species where no ambiguities exist. Calculation of the fractional cross sections $C_2D_3^+$, $C_2H_3^+$ at 1.7 eV collision energy reveals that even in this worst-case situation the contribution of $C_2D_3^+$ to the $C_2H_4D^+$ product intensity is less that 25%, within the overall uncertainty of the cross sections as indicated by the error bars in Figure 2a.

Results

Probability contour plots in Cartesian velocity space for products from reactions 1a and 1b are shown at several collision energies in Figure 1. The product distributions are peaked clearly forward of the center-of-mass (CM) with no evidence of forward–backward symmetry. Thus the direct mechanism reported by Herman,[1] *et al.*, is confirmed for all labeled products.

The following procedure has been used to calculate relative total cross sections from contour plots and product mass spectra measured at a fixed laboratory angle. First, in order to integrate conveniently over the intensity volume, it is necessary to convert the probability contours in Cartesian coordinates to intensity contours in CM coordinates. Thus[7]

$$I_{lab}/v^2 = P_c(v_x,v_y,v_z) = P_c'(u_x,u_y,u_z) = I_{cm}/u^2$$

where $P_c(v_x,v_y,v_z)$ and $P_c'(u_x,u_y,u_z)$ are probability functions of Cartesian space, u is the CM velocity coordinate, v is the laboratory (LAB) velocity coordinate, I_{cm} is the product intensity in CM velocity space, and I_{lab} is the product intensity in LAB velocity space. The total cross section can be written in terms of the probability contour map as

$$\sigma = \int_0^{\pi}\int_0^{2\pi}\int_0^{\infty} P_c'(u_x,u_y,u_z)u^2 \sin\theta \, du d\phi d\theta = 2\pi\int_0^{\pi}\int_0^{\infty} I_{cm}(u,\theta)\, du \sin\theta \, d\theta \quad (2)$$

where θ and ϕ are the CM polar and azimuthal angles, respectively. Note that in CM coordinates the product intensity volume is symmetric about the reactant relative velocity vector; and, therefore, integration over ϕ (out-of-plane scattering) is simply a constant factor of 2π. Note also that the contour values in Figure 1 have been normalized to the peak value for each contour map. In order to obtain the relative magnitude of the cross sections for each isotopic product, it is necessary to relate the observed product mass spectra, S' (measured at a fixed LAB angle of 3° with respect to the reactant ion beam), to the self-normalized probability contour plots for each isotopic product. To do this we write a calculated mass spectral intensity, S, for an isotopic product as the integrated LAB intensity distribution over all energies at a fixed LAB angle in the plane of the two reactant beams

$$S = \int_0^{\infty} I_{lab}(E_{lab},3°,0)\ dE_{lab} = \int_0^{\infty} I_{lab}(v,3°,0)\ dv$$

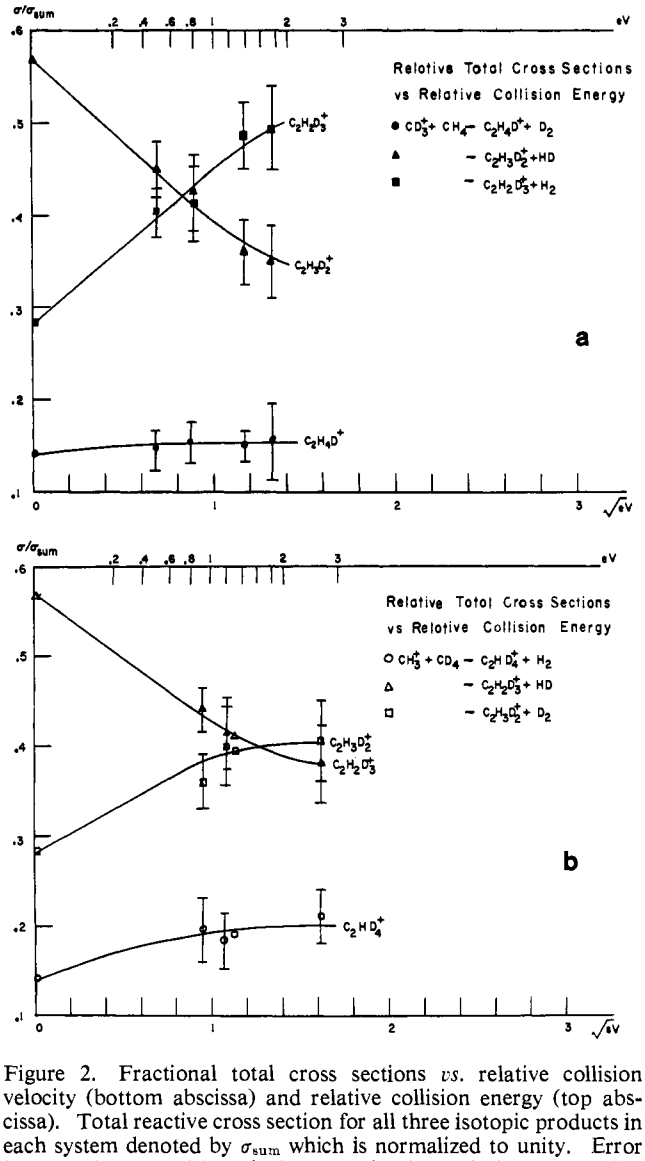

Figure 2. Fractional total cross sections *vs.* relative collision velocity (bottom abscissa) and relative collision energy (top abscissa). Total reactive cross section for all three isotopic products in each system denoted by σ_{sum} which is normalized to unity. Error bars on data at 1.26 eV in b are omitted for clarity. Note that points at zero energy are calculated assuming random scrambling.

where m is the mass of the isotopic product and v is LAB velocity coordinate. Then, since $I_{lab}(v,3°,0) = v^2P_c(v_x,v_y,v_z)$ it follows that

$$S = \int_0^{\infty} v^2 P_c(v_x,v_y,v_z)\, dv \quad (3)$$

The integral on the right of eq 3 can be calculated directly from the contour plots. The ratio of the measured intensity, S', to S provides the appropriate factor for scaling the integral on the right side of eq 2. Therefore, the relative total cross section is given by

$$\sigma_{rel} = (S'/S)\sigma \quad (4)$$

Graphs of the isotopic relative cross sections (normalized to their sum in each system) as a function of collision energy and velocity are presented in Figure 2. Clearly the trend in both systems is toward nonrandom scrambling with increasing collision energy.

Errors in the final cross sections arise from two main sources: uncertainty in the construction of the probability contour maps and noise in the measured mass spectral data. Because the reactant beams have small angular divergences and are not monoenergetic, a

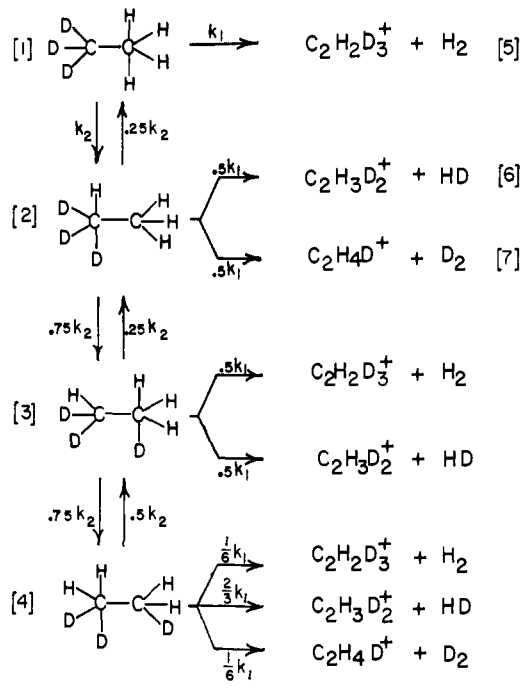

Figure 3. The kinetic model proposed to explain nonrandom scrambling. Rate constants k_1 and k_2 are weighted by statistical probabilities, assuming H and D to be equivalent particles (no isotope effects). The model, as shown, is appropriate for reaction 1a. The complementary reaction, 1b, is described by interchanging H's and D's.

unique center-of-mass cannot be located on a contour map. Distributions in energy and angle of the reactant beams result in a distribution of centers-of-mass. We have chosen to use the most probable reactant laboratory velocity vectors in order to determine a most probable center-of-mass. Uncertainty in the center-of-mass location becomes more important at higher energies since the probability contours peak closer to the center-of-mass as collision energy increases (compare Figures 1a and 1b and 1c and 1d). Reactant beam intensity, however, is improved at higher collision energies; and therefore uncertainty in the relative intensities of the product mass spectra is much reduced. Thus the combined uncertainty from the calculation of σ (eq 2) and the measurement of S' remains roughly constant over the entire energy range. A third but relatively minor source of error is in the calculation of S from eq 3. The LAB velocity vector required for the integration is obviously much less sensitive to small changes in the location of the product contour map along the relative velocity vector than is the CM velocity vector. The combined uncertainty in σ_{rel} from each of the above sources (assuming no correlation between them) is

$$\frac{(\delta\sigma_{rel})^2}{\sigma_{rel}^2} = \frac{(\delta\sigma)^2}{\sigma^2} + \frac{(\delta S)^2}{S^2} + \frac{(\delta S')^2}{S'^2} \qquad (5)$$

In practice the overall uncertainty has been calculated by determining σ, S, and S' several times at each collision energy, then calculating their averages and standard variances. Equation 5 is then used to calculate the standard variances in σ_{rel} which in turn determine the error bars in Figure 2.

Kinetic Model

Since the contour plots for all three product ions in each isotopic system have closely similar features, it is reasonable to presume that all product ions result from the same mechanism and emerge from the same intermediate. Both present and previous work[1] have established a direct mechanism with forward peaking over the range 0.52–3.46 eV collision energy. Forward peaking of the products together with a large reaction cross section generally characterize a stripping or pick-up mechanism. In the present case the incoming ion reacts with neutral methane by "picking up" a methylene fragment and leaving H_ND_{2-N} (N = 0, 1, 2) behind. However, extensive hydrogen–deuterium scrambling in the products indicates that the time required for pick-up to occur is long compared with the time it takes hydrogens to jump back and forth between the two carbon atoms. It is quite reasonable, therefore, to picture the hydrogen–deuterium exchange occuring through a $C_2H_ND_{7-N}^+$ (N = 3, 4) collision intermediate which is short-lived with respect to a few rotational periods but well-defined with respect to hydrogen–deuterium interchange.

In keeping with this general picture we propose a simple model for the reaction. Figure 3 shows the kinetic scheme we have chosen to describe the processes involved. Note that Figure 3 is appropriate to reaction 1a. To describe reaction 1b, H's and D's must be interchanged. A rate constant, k_1, is assigned to the dissociation of $C_2H_ND_{7-N}^+$ into the $C_2X_5^+ + X_2$ (X = H, D) products, ignoring any isotope effects on the dissociative rate. A second rate constant, k_2, is assigned to intramolecular proton or deuteron transfer (scrambling) processes occurring in the intermediate, again ignoring any isotope effect.[8a,b] The *relative* rates of the two competing processes, dissociation and scrambling, then determine the isotopic distribution in the final products. The kinetics scheme is described mathematically by writing down a first-order rate equation for each of the numbered species in Figure 3. The result is a set of coupled first-order differential equations. The initial "concentrations" are specified (concentration of species I is set equal to unity; all other initial concentrations are set equal to zero), and the rate equations are solved using the matrix technique outlined in Appendix A. The procedure is repeated over a range of relative values for k_1 and k_2 and the results are compared with the experimentally determined total cross sections. Figure 4 illustrates the ability of the kinetic model to reproduce the observed nonrandom product distributions (Figure 2). Note that the model uses one parameter, the ratio of k_1 to k_2, to fit the cross-section data. The results of the model calculations are consistent with our previous physical picture. At low energy the collisional interaction time is long enough to permit many H–D jumps before the intermediate dissociates to final products. As collision energy increases, fewer jumps are permitted before dissociation. This situation corresponds to a smoothly increasing value for the rate of dissociation relative to scrambling.

(8) (a) Although isotope effects are undoubtedly present (see Discussion section), the simplicity of the model precludes any meaningful *quantitative* estimate of the difference between scrambling and dissociation rates for hydrogen and deuterium. To attempt such an inappropriate refinement would merely cloud the issue by introducing another independently adjustable parameter. (b) ". . . For it is the mark of an educated man to look for precision in each class of things just so far as the nature of the subject admits . . .," Aristotle, "Ethics," Book I.

Discussion

Two assumptions are implicit in our kinetic scheme. First, the "extra" proton (or deuteron) in the hypercoordinated carbonium ion intermediate is associated with one carbon atom or the other, but does not form a bridge between the two. In other words (for reaction 1a) we prefer the structure I with a pentacoordinated carbon atom over structure II.

$[CD_3—CH_4]^+$ (I)

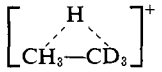

(II)

Justification for our preference can be inferred from the relative magnitudes of the reaction cross sections. If the reaction proceeded through symmetrical structure II, then one would expect a nonrandomized product distribution to reflect this symmetry, *i.e.*, show either equal intensities of $C_2H_3D_2^+$ and $C_2H_2D_3^+$ (if the bridging hydrogen participated in the dissociation) or equal intensities of $C_2H_4D^+$ and $C_2H_2D_3^+$ (if the bridging hydrogen did not participate in the dissociation). Contrary to these expectations, we find that $C_2H_2D_3^+$ predominates over $C_2H_3D_2^+$ as the product intensity distributions become nonrandom, a result consistent with structure I. Results for reaction 1b support structure I′ (structure I with D's and H's interchanged).

$[CH_3—CD_4]^+$ (I′)

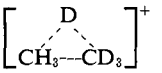

(II′)

Figure 2b shows that $C_2H_3D_2^+$ predominates over $C_2H_2D_3^+$ with increasing collision energy, consistent with our expectation. It is clear from Figure 2, however, that the two isotopic systems do not show identical behavior. Note that in Figure 2b the cross section for $C_2H_3D_2^+$ appears to be somewhat smaller and the cross sections for $C_2H_2D_3^+$ and $C_2HD_4^+$ somewhat larger than their counterparts in reaction 1a. This isotope effect may be rationalized by invoking Wolfgang's golden rule[9] which states that "... reactions requiring nuclear motions which are slow relative to the time of collision tend to be forbidden." Clearly the bending vibration in CD_4 necessary to accommodate the incipient structure I′ will be slower than the corresponding motion of CH_4 necessary for the formation of structure I. It is possible, therefore, that in the case of reaction 1b a deuterium nucleus, responding more slowly to the time-dependent force of the incoming CH_3^+ ion, will find itself "delocalized" between the two carbon nuclei as the carbon–carbon bond begins to form. Such a circumstance would effectively result in the enhancement of the dissociative rates for $C_2HD_4^+$ and $C_2H_2D_3^+$ production relative to $C_2H_3D_2^+$. Thus as the total time of collision is decreased (collision energy increased), a structure such as II′ may become increasingly important due to what may be termed an inertial or "kinematic" isotope effect.

Our second assumption is that decomposition of the intermediate always takes place from the pentacoordinated carbon. Presumably the pentacoordinated carbon is more likely to split off H_ND_{2-N} ($N = 0, 1, 2$). The resulting product is then a normal ethyl cation. Furthermore, the hydrogens and deuteriums associated with the pentacoordinated carbon should all be closer to each other than to the other carbon atom; and therefore a "1, 1 elimination" from the pentacoordinated carbon appears more likely than a "1, 2 elimination" across the molecule.

(9) R. Wolfgang, *Progr. React. Kinet.*, 3, 137 (1965).

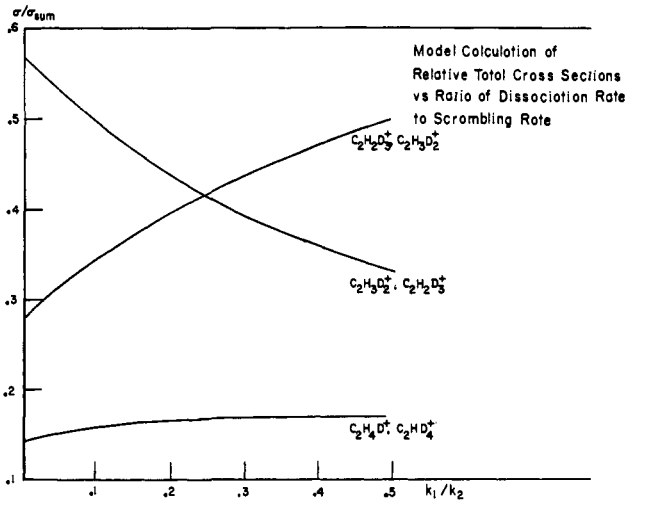

Figure 4. Fractional total cross sections *vs.* k_1/k_2 calculated from model shown in Figure 3.

Table I. Relative Collision Energy *vs.* the Ratio of the Dissociation Rate Constant, k_1, to the Scrambling Rate Constant, k_2[a]

Collision energy, eV	0.50	0.80	1.1	1.4	1.7
k_1/k_2	0.17	0.22	0.26	0.28	0.32

[a] The k_1/k_2 ratios were chosen so as to give best model fit to product ion cross sections as a function of energy for reactions 1a and 1b.

Recently much study has been devoted to possible structures for cations with pentacoordinated carbon atoms.[10–12] We believe that the crossed-beam technique can be a powerful tool for probing the structural and dynamical behavior of carbonium ion intermediates.

It is also worth noting that although the model we have proposed yields only the ratio of the dissociation rate to the scrambling rate, it is also possible to obtain an estimate of the absolute scrambling rate by recourse to simple theories of unimolecular decay.[13] A previous calculation by Herman,[1] *et al.*, estimated the dissociative rate to be $\lesssim 1 \times 10^{13}$ sec^{-1}. This estimate is confirmed by a later and more positive determination[14] of the thermochemical data for $C_2H_7^+$. From our ratio k_1/k_2, therefore, we may estimate an upper limit to the absolute scrambling rate to lie in the range between 10^{13} and 10^{14} sec^{-1}.

Table I compares the k_1/k_2 ratios with relative collision energy over the range covered by this study. The values of k_1/k_2 have been assigned to collision energies so as to give the best overall data fit to the product cross sections for systems 1a and 1b. Note that an approximately

(10) G. A. Olah, *J. Amer. Chem. Soc.*, 94, 808 (1972), and references therein.
(11) J. Weiner, A. Lee, and R. Wolfgang, *Chem. Phys. Lett.*, 13, 613 (1972).
(12) M. Saunders, P. Vogel, E. L. Hagen, and J. Rosenfeld, *Accounts Chem. Res.*, 6, 53 (1973).
(13) L. S. Kassel, "Kinetics of Homogeneous Gas Reactions," Chemical Catalog Co., New York, N. Y., 1932.
(14) S.-L. Chong and J. L. Franklin, *J. Amer. Chem. Soc.*, 94, 6347 (1972).

fourfold increase in collision energy results in a twofold increase in k_1/k_2. This may mean that the dissociation rate varies reciprocally with the relative velocity, *i.e.*, depends directly on a "time of collision." If it is assumed that the scrambling rate, k_2, is insensitive to collision energy, then one would expect k_1/k_2 to vary with the square root of relative energy as indicated by the data in Table I The RRK theory of unimolecular dissociation, while providing an estimate of the intermediate lifetime, appears to be rather inappropriate to this system. The exceedingly small "well depth" of $C_2H_7^+$ relative to $C_2H_5^+ + H_2$ (0.2 kcal/mol) allows little time for energy equilibration among internal modes and results in a dissociation rate insensitive to any collision energy dependence.

Several avenues for further investigation immediately present themselves. Decomposition of $C_2X_5^+$ (X = H, D) products into $C_2X_3^+$ (X = H, D) becomes an important process above 1.2 eV collision energy. It is a straightforward matter to extend the model to include the $C_2X_3^+$ products in the previous decomposition scheme. The question of isotope effects may be further investigated by studying other isotopic combinations, such as

$$CH_3^+ + CH_3D \begin{cases} \longrightarrow C_2H_5^+ + HD \\ \longrightarrow C_2H_4D^+ + H_2 \end{cases}$$

or

$$CD_3^+ + CHD_3 \begin{cases} \longrightarrow C_2D_5^+ + HD \\ \longrightarrow C_2HD_4^+ + D_2 \end{cases}$$

Both of these questions are presently under investigation.

Acknowledgment. The financial support of the National Aeronautics and Space Administration and the National Science Foundation (grant to M. S.) is gratefully acknowledged.

Appendix A

In order to apply the kinetic model of scrambling and dissociation presented in the text, one must solve a set of coupled first-order rate equations. This was first accomplished in this work by direct numerical integration of the differential equations using an interactive computer program written by one of us (M. S.) and employing the Runge-Kutta procedure; or, alternatively, one may uncouple the rate equations by writing the set in matrix form, diagonalizing the isotopic scrambling matrix, and integrating the resulting uncoupled set of equations analytically. These two methods were shown to produce equivalent results. The latter procedure was used to calculate final product intensities as a function of k_1/k_2, the ratio of dissociation rate to scrambling rate.

The coupled rate equations are written

$$\dot{A}_i = \sum_{j=1}^{N} C_{ij}k_2A_j - k_1A_i \tag{1A}$$

$$\dot{B}_l = \sum_{k=1}^{N} E_{lk}k_1A_k \tag{2A}$$

where the set of $\{A_i\}$ are the different isotopic arrangements of $C_2X_7^+$ (X = H, D) intermediate (species 1–4 in Figure 3), and $\{B_l\}$ are the set of final reaction products (species 5–7 in Figure 3). The matrix elements C_{ij} and E_{lk} represent the probability that a given proton rearrangement or dissociation of species j or k will produce species i or l. Examples of these matrix elements are the rate constant coefficients in Figure 3. The constants k_1 and k_2 are the overall dissociation and scrambling rate constants, respectively. We assume that the rate constants are insensitive to the mass difference between hydrogen and deuterium, that all H's (and D's) are equivalent, but that H's and D's can be distinguished from each other. With these assumptions we write C_{ij} as the statistical probability that species i can be formed from species j in a single proton (deuteron) jump. Then, from microscopic reversibility

$$\frac{C_{ij}}{C_{ji}} = \frac{W_j}{W_i} \tag{3A}$$

where W_i is the statistical weight (*i.e.*, the probability of formation in a randomized system) of species i. In Figure 3 the statistical weights for species 1–4 are 1, 4, 12, and 18, respectively. The rate law for unimolecular decay of the intermediate is expressed as

$$A_i = A_0y_ie^{-k_1t} \tag{4A}$$

where A_0 is the initial concentration and y_i is the mole fraction of species i. Defining

$$x_i(t) \equiv y_i(t)/(W_i)^{1/2} \tag{5A}$$

we substitute (5A) and (4A) into (1A) so that

$$\dot{x}_i = k_2 \sum_{j=1}^{N} D_{ij}X_j$$

where

$$D_{ij} = C_{ij}(W_j/W_i)^{1/2} \tag{6A}$$

or in matrix notation

$$\dot{\mathbf{x}} = k_2\mathbf{D}\mathbf{x} \tag{7A}$$

From (3A), (5A), and (6A), we see the **D** matrix is Hermitian and therefore has real eigenvalues and is diagonalized by some unitary matrix, **T**. Let

$$\mathbf{z} = \mathbf{T}\mathbf{x} \tag{8A}$$

so that (7A) becomes

$$\dot{\mathbf{z}} = k_2(\mathbf{T}\mathbf{D}\mathbf{T}\dagger)\mathbf{z} = k_2\mathbf{D}'\mathbf{z} \tag{9A}$$

where $\mathbf{D}'$ is the diagonalized matrix. Integrating (9A) for a particular element, m

$$z_m(t) = z_m(0)e^{D'_{mm}k_2t}$$

so that from (8A)

$$x_i(t) = \sum_{m,j} T\dagger_{im}T_{mj}x_j(0)e^{D'_{mm}k_2t} \tag{10A}$$

Substituting (10A), (5A), and (4A) into (2A)

$$\dot{B}_l = \sum_{i,m,j} E_{lj}T\dagger_{im}T_{mj}k_1A_0y_j(0)\left(\frac{w_i}{w_j}\right)^{1/2} e^{(D'_{mm}k_2-k_1)t} \tag{11A}$$

Finally, integrating B_l over all time gives the final product concentrations

$$B_l(t=\infty) = \sum_{i,m,j} E_{lj}T\dagger_{im}T_{mj}A_0y_i(0)\left(\frac{w_i}{w_j}\right)^{1/2} \Big/ (1 - D'_{mm}k_2/k_1) \tag{12A}$$

Note that the solutions $B_l(t=\infty)$ depend only on the initial concentrations, $[A_0,y_j(0)]$, and the ratio of the rate constants, k_2/k_1. Thus the **D** matrix need only be diagonalized once for all final product concentrations over an arbitrary range of rate-constant ratios.